No. 1A-1 $NaNbO_3$, Sodium niobate

(M = 163.89)

1a In 1951 Matthias et al. found dielectric anomalies in $NaNbO_3$ and proposed the crystal to be considered ferroelectric. In 1955, however, Cross et al. proved that it is antiferroelectric at room temperature and expected that it is ferroelectric below about −200 °C based on their observation of its complicated dielectric behaviors. 51Mat 55Cro

b

phase	V	IV	III''	III'	III	II	I
state	(F)	A					P
crystal system	trigonal [a])	ortho-rhombic [b])	ortho-rhombic [c])	ortho-rhombic [d])	ortho-rhombic [d])	tetragonal	cubic
space group	R3c– C_{3v}^{6} [a])	Pbma– D_{2h}^{11} [b])	Pmnm– D_{2h}^{13} [c])	Pnmm– D_{2h}^{13} [d])	Ccmm– D_{2h}^{17} [d])	P4/mbm– D_{3h}^{5} [e])	Pm3m– O_{h}^{1} [g])
Θ [°C]	−200	365 [f])	480 [f])	520 [f])	572 [f])	643 [f])	

[a]) 71Dar
[b]) 61Wel
[c]) 71Sak
[d]) 72Aht
[e]) 72Gla
[f]) 73Ish
[g]) 51Woo

When a field of which strength exceeds a threshold value is applied parallel to b-axis below −120 °C in phase IV, normal hysteresis loop appears, implying a ferroelectric phase is induced.

Phases II, III, III', III'', IV and V are called T_2, T_1, S, R, P and N, respectively, in some original papers. 72Aht

2 Crystal growth:

Cooling method from a molten mixture of Na_2CO_3, Nb_2O_5 and NaF. 51Woo

Top-seeded solution technique. 74Daw

See also 80Smo

3a Unit cell parameters:

phase II: a = 5.5639(6) Å ≈ $\sqrt{2}a_0$, 72Gla
b = 5.5639(6) Å ≈ $\sqrt{2}a_0$,
c = 3.9428 (4) Å ≈ a_0 at 600 °C.

phase III: a = 7.8642 Å ≈ $2a_0$, 72Aht
b = 7.8550 Å ≈ $2a_0$,
c = 7.8696 Å ≈ $2a_0$ at 530 °C.

phase III': a = 7.8608 Å ≈ $2a_0$, 72Aht
b = 7.8556 Å ≈ $2a_0$,
c = 7.8606 Å ≈ $2a_0$ at 500 °C.

phase III'': $a \approx 2a_0$, 71Sak
$b \approx 6a_0$,
$c = 2a_0$ at T > 365 °C.

phase IV: $a = c = 2 \cdot 3.9150(2)$ Å, 73Dar
$b = 4 \cdot 3.8798$ (2) Å,
$\alpha = \gamma = 90°$,
$\beta = 90°40(3)'$ at RT.

phase V: $a = b = c = 2 \cdot 3.9083(5)$ Å, 73Dar
$\alpha = 89°13(1)'$ at −150 °C. *)

a_0: lattice parameter of cubic cell in phase I.

In phase IV (orthorhombic system) the longest edge of a unit cell was taken as b-axis by Well and Megaw.

This system of axes is adopted throughout the present description. In an original paper 61Wel

	given by Vousden, *b*- and *c*-axes were interchanged. *) The phase V is metastable at –l50 °C.	51Vou
b	Crystal structures:	
	phase II: $Z = 2$	72Gla
	Approximate structure has been studied by Glazer et al. [a]) and Ishida et al. [b]). Essentially the same results have been obtained: Table 1A-1-001.	[a]) 72Gla [b]) 73Ish
	phases III and III': $Z = 8$. Table 1A-1-001; Fig. 1A-1-001.	72Aht
	phase III'': $Z = 24$.	71Sak
	phase IV: $Z = 8$. Table 1A-1-002; Fig. 1A-1-002. Interatomic distances: Table 1A-1-003. Atomic displacement: Table 1A-1-004, 1A-1-005.	61Wel
	phase V: $Z = 2$. Table 1A-1-006.	71Dar
4	Lattice distortion: For phases I, II, III, III', III'': Fig. 1A-1-003. For phase V: see	73Dar
5a	Dielectric constant: Fig. 1A-1-004. Curie-Weiss law: $\kappa = C / (T - \Theta_p)$, $T > \Theta_{IV-III''}$, where $C = 2...4 \cdot 10^5$ K and $\Theta_p = 60...80$ °C. Pressure effect: Fig. 1A-1-005, Fig. 1A-1-006. Phase transformation under high electric field: Figs. 1A-1-008, 1A-1-009, 1A-1-010; Table 1A-1-007. Frequency dependence: see Effect of Mn additives (ceramics): see	54Shi 79Tur 85Mol, 88Mol, 94Mol
c	Spontaneous polarization: $P_s \approx 0.12$ Cm^{-2} in the field-induced ferroelectric phase. See also 1b.	55Cro
d	Pyroelectric effect: see	79Rae, 81Pro
9a	Refractive indices in phase IV: $n_\alpha = 2.13(2)$, $n_\beta = 2.21(2)$, $n_\gamma = 2.25(2)$, $2V = 109(4)^o$ for $\lambda = 589$ nm. Birefringence: Figs. 1A-1-011, 1A-1-012, 1A-1-013. Infrared reflectivity: Fig. 1A-1-014.	78Sei
11	Forbidden band width was estimated to be 3.4 eV from the wavelength dependency of photoconductivity. Dark conductivity: $\sigma_d \approx 5 \cdot 10^{-12}$ $\Omega^{-1} m^{-1}$ at 295 K. Thermoelectric effect: Fig. 1A-1-015; see also Hall coefficient and thermoelectric power between 70 and 300 K: see AC conductivity at low frequencies: see Band structure: see	77Rae1 77Rae2 78Han 80Tan 91Bak 94Kin
13a	NMR: Figs. 1A-1-016, 1A-1-017, 1A-1-018; see also	74Avo
b	ESR: Spin Hamiltonian parameters: $g = 2.003(2)$, $E = 80(3) \cdot 10^{-2}$ m^{-1}, $A = -81.5(20) \cdot 10^{-2}$ m^{-1} at RT. Table 1A-1-018; see also ESR for the crystal doped with Mn^{2+}: see	75Gei 84Mol 76Gei

14a	Superlattice X-ray reflections: Fig. 1A-1-019, Fig. 1A-1-020.	
b	Diffuse X-ray scattering: see	71Com, 73Ish
	Inelastic neutron scattering: Fig. 1A-1-021.	
15a	Domain structure: see	55Cro, 64Per, 62Mil, 62Woo, 83Zhe, 88Che, 88Dec
b	Dynamic properties: Fig. 1A-1-022, Fig. 1A-1-023.	

Table 1A-1-001. $NaNbO_3$. Fractional coordinates of atoms in phases II, III and III'.

Phase III' [a])		Phase III [a])		Phase II [b])	
Nb(1) in 4(c)	0, 0, 0	Nb in 8(d)	0, 0, 0	Nb 2(a):	0, 0, 0; ½, ½, 0
Nb(2) in 4(d)	½, 0, 0			Na 2(c):	0, ½, ½, ½; ½, 0, ½
				O(I) 2(b):	0, 0, ½; ½, ½, ½
Na(1) in 2(a)	¼–t_1, ¼, ¼	Na(1) in 4(c)	¼–t_1, ¼, ¼	O(II) 4(g):	¼+x_1, ¼–x_1, 0;
Na(2) in 2(a)	¾–t_2, ¼, ¼	Na(2) in 4(c)	¾–t_2, ¼, ¼		¾+x_1, ¼+x_1, 0;
Na(3) in 2(b)	¾–t_3, ¾, ¼				¾–x_1, ¾+x_1, 0;
Na(4) in 2(b)	¼–t_4, ¾, ¼				¼–x_1, ¾–x_1, 0;
O(1) in 8(g)	0.25, –0.013, –0.009	O(1) in 8(e)	¼, –0.015, 0		
O(2) in 4(f)	0.013, ¼, –0.013	O(2) in 8(f)	0.015, ¼, –0.012		
O(2') in 4(f)	0.487, ¼, 0.013				
O(3) in 4(e)	0.009, 0.013, ¼	O(3) in 8(g)	0, –0.012, ¼		
O(3') in 4(e)	0.491, –0.013, ¼				
$t_1 = t_2 \approx 0$		$t_1 = t_2 < 0.014$		$x_1 = x_2 \approx 0.015$	
$t_3 = t_4 < 0.02$					
T = 500 °C		T = 530 °C		T = 600 °C	

[a]) [72Aht]. [b]) [72Gla].

Table 1A-1-002. $NaNbO_3$. Fractional coordinates and temperature parameters in phase IV [69Sak]. B_{ij} is defined by Eq. (a) in Introduction.

	Nb	Na(l)	Na(2)	O(1)	O(2)	O(3)	O(4)
x	0.2722(2)	0.750	0.782(3)	0.250	0.233(3)	0.032(2)	0.467(2)
y	0.1262(2)	0	0.250	0	0.250	0.140(1)	0.110(1)
z	0.2566(1)	0.243(2)	0.239(2)	0.304(3)	0.191(3)	0.536(1)	0.966(1)
B_{11}	0.0021(2)	0.0246(85)	0.0086(31)	0.0011(40)	0.0009(24)	0.0008(15)	0.0093(29)
B_{22}	0.0004(0)	0.0018(8)	0.0007(4)	0.0003(5)	0.0004(5)	0.0008(3)	0.0007(4)
B_{33}	0.0023(1)	0.0064(41)	0.0072(36)	0.0089(27)	0.0064(23)	0.0033(12)	0.0018(10)
B_{12}	–0.0006(1)	–0.0009(11)	0	–0.0006(7)	0	0.0007(6)	0.0015(8)
B_{13}	–0.0004(2)	0	–0.0051(24)	0	0.0024(25)	0.0013(13)	0.0022(16)
B_{23}	–0.0003(1)	0	0	0	0	0.0002(5)	0.0004(4)

Table 1A-1-003. $NaNbO_3$ (phase V (N) and phase IV (P)), $LiNbO_3$, $KNbO_3$. Interatomic distances.

Formula Nb displacement	$NaNbO_3$ (N) [a] 0.23	$NaNbO_3$ (P) [b] 0.13	$LiNbO_3$ [c] 0.26	$KNbO_3$ (ortho) [d] 0.20
Nb–O	1.862(2)	1.903 *)	1.889	1.863
	2.122(3)	1.974 *)	2.112	1.991
		2.080 *)		2.180
A–O	2.42(3)	2.421 *)	2.068	2.792
(A = Na, Li, K)	2.56(8)	2.785 *)	2.238	2.854 *)
	3.05(10)	3.088 *)		2.873
	3.10(3)			
		2.440 *)		
		2.699 *)		
		3.140 *)		
O–O	2.803(8)	2.795 *)	2.719	2.780 *)
	2.806(11)	2.798 *)	2.801	2.854 *)
		2.814 *)	2.840	2.884 *)
			2.879	
	2.804 *)	2.802 *)	2.810 *)	2.839 *)

[a]) [73Dar]. [b]) [69Sak]. [c]) [66Abr]. [d]) [67Kat].

*) Bonds included are not all symmetry-equivalent, and the length given is a mean value.

Table 1A-1-004. $NaNbO_3$. Atomic coordinates in phase IV [74Hew]. u ,υ ,w indicate the displacements from cubic perovskite position.

Nb	8(e)	¼ + u_{Nb}	1/8 + υ_{Nb}	¼ + w_{Nb}
Na1	4(c)	¾	0	¼ + w_{Na1}
Na2	4(d)	¾ + u_{Na2}	¼	¼ + w_{Na2}
O1	4(c)	¼	0	¼ + w_{O1}
O2	4(d)	¼ + u_{O2}	¼	¼ + w_{O2}
O3	8(e)	u_{O3}	1/8 + υ_{O3}	½ + w_{O3}
O4	8(e)	½ + u_{O4}	1/8 + υ_{O4}	w_{O4}

Table 1A-1-005. $NaNbO_3$. Atomic displacements in phase IV. **(a)**: X-ray single crystal analysis [69Sak], **(b)**: neutron powder profile refinement [74Hew]. Temperature parameter β_{ij} is defined by Eq. (c) in Introduction.

(a) X-ray structure:

	u	*v*	*w*
Nb	0.0222(2)	0.0012(2)	0.0066(1)
Na1	0	0	–0.007(2)
Na2	0.032(3)	0	–0.011(2)
O1	0	0	0.054(3)
O2	–0.017(3)	0	–0.052(3)
O3	0.032(2)	0.0150(10)	0.036(1)
O4	–0.033(2)	–0.0150(10)	–0.034(1)

(b) Neutron structure:

	u	*v*	*w*
Nb	±0.0205(7)	0.0019(6)	∓0.003(2)
Na1	0	0	±0.007(4)
Na2	±0.031(2)	0	±0.004(4)
O1	0	0	±0.054(2)
O2	∓0.018(2)	0	∓0.070(2)
O3	±0.025(1)	0.0160(4)	±0.033(1)
O4	∓0.044(1)	0.0160(4)	∓0.036(1)
	β_{11}	β_{22}	β_{33}
Nb	0.4(1)	0.7(1)	0.4
Na1, Na2	1.0(2)	1.6(2)	1.0
O1, O2	1.2(1)	0.9	1.2
O3, O4	0.6(1)	1.2	0.6
O3, O4		β_{13} = 0.3(1)	

a = 5.5679(3) Å, b = 15.5156(8) Å, c = 5.5029(3) Å

The upper set of double signs for the neutron parameters refer to the (+) solution and the lower set to the crystallographically equivalent (–) solution, which is obtained by reversing the x and z axes and interchanging the 03 and 04 displacements. X-ray structure gives R = 0.085 with neutron powder data, whereas neutron structure gives R = 0.046 with that.

Table 1A-1-006. $NaNbO_3$. Fractional coordinates and temperature parameters in phase V (−150 °C) [73Dar]. Atomic positions are given referring to the pseudocubic axes. *B* is defined by Eq. (e) in Introduction.

Na	(s, s, s)	Na	s = 0.272(8)	*B*(Na) = l.0 Å^2
Nb	(t, t, t)	Nb	t = 0.016(3)	*B*(Nb) = 0.66 Å^2
O	(−e+d, ¼−2d, e+d)	O	e = 0.031(4)	*B*(O) = 0.6 Å^2
			d = 0.0	

Table 1A-1-007. $NaNbO_3$. Characteristics of field-induced phase transitions [90Uli]. ΔP: projection of the polarization step along applied field direction, dE/dT: slope of the transition line (phase boundary in E–T diagram), ΔQ: latent heat calculated according to Clausius-Clapeyron relation $\Delta Q = -T\,(dE/dT)\,\Delta P$.

Phase transition	T [K]	ΔP [10^{-2} Cm^{-2}]	dE/dT [10^5 $Vm^{-1}K^{-1}$]	ΔQ [$Jmol^{-1}$]
Pbma → $P2_1ma$	293	11.4	–0.63	75
$P2_1ma$ →tetragonal	293	–0.5	–4.2	22.1
Pbma → R3c	146	11.7	2.06	–126

Table 1A-1-008. $NaNbO_3$. Spin Hamiltonian parameters [82Gei]. Mn^{2+} center located at Na-site.

T [K]	g	D [10^{-2} m^{-1}]	E [10^{-2} m^{-1}]	A [10^{-2} m^{-1}]
653	2.002(2)	275(5)	<40	–78.6(3)
300	2.022			–83(2)
77	2.000(3)	277.3(4)		–83(3)

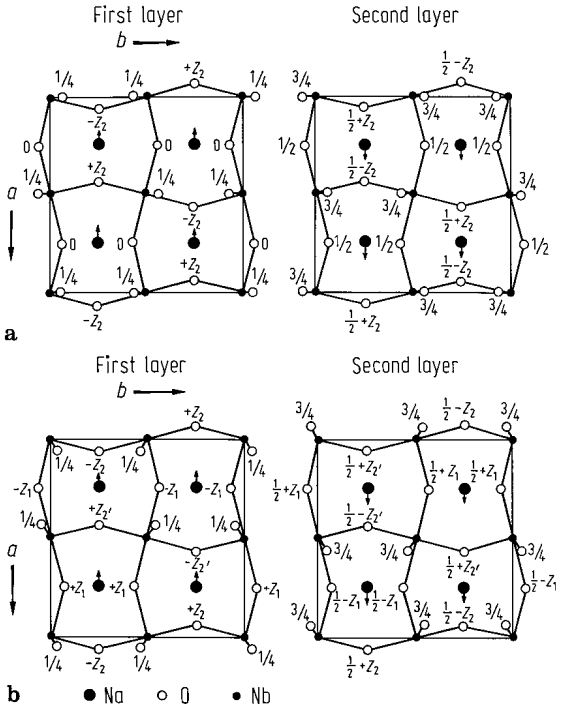

Fig. 1A-1-001. $NaNbO_3$. Structure of phases III and III' [72Aht]. Projections on (001) plane. **(a)**: phase III, **(b)**: phase III'. Heights of oxygen atoms above the (001) plane through the origin are given in the figure. Directions and relative magnitudes of possible displacement of Na are indicated by arrows.

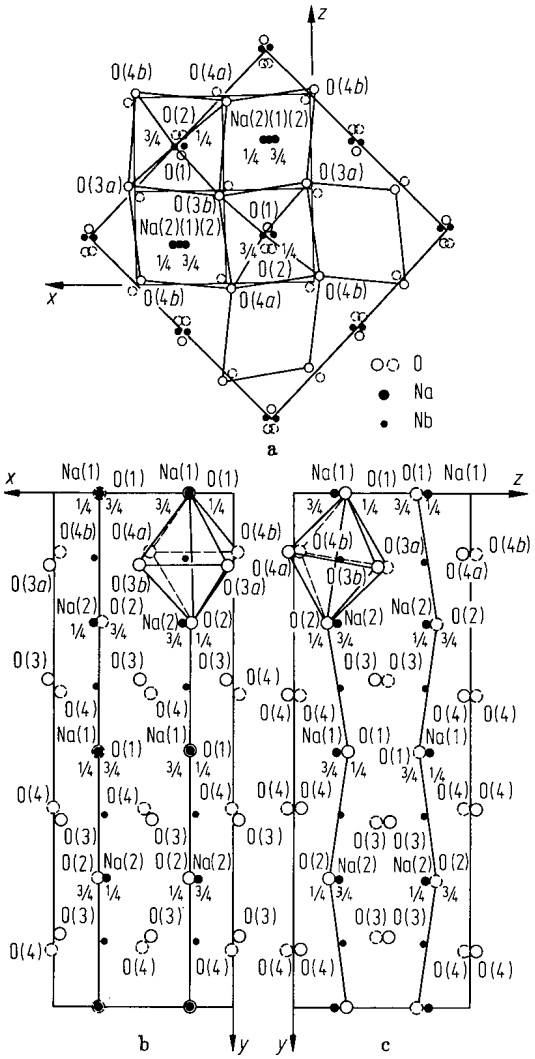

Fig. 1A-1-002. $NaNbO_3$. Structure of phase IV [69Sak]. **(a)**: projection on (010), **(b)**: projection on (001), **(c)**: projection on (100). See also Table 1A-1-002.

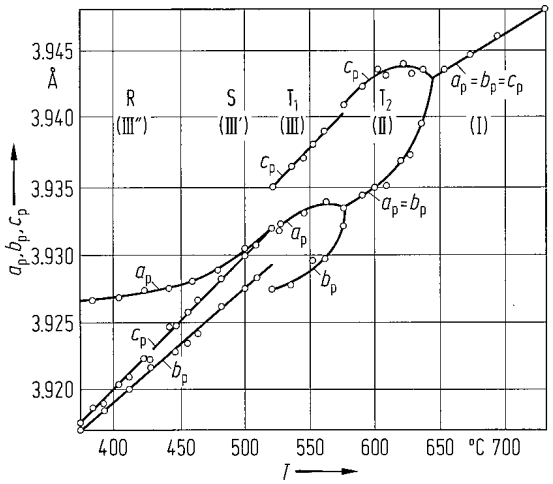

Fig. 1A-1-003. $NaNbO_3$. a_p, b_p, c_p vs. T [72Aht]. a_p, b_p, c_p: pseudocubic lattice parameters.

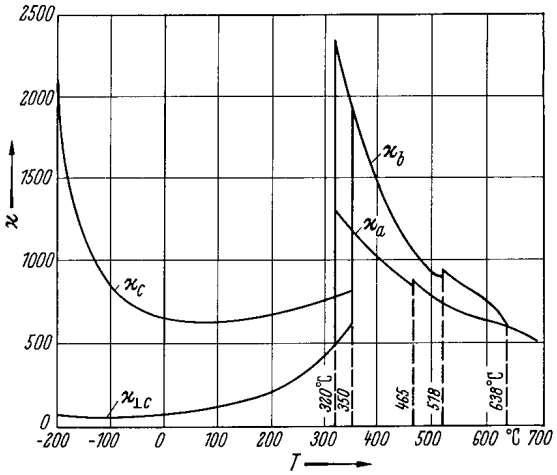

Fig. 1A-1-004. $NaNbO_3$. κ_a, κ_b, κ_c, $\kappa_{\perp c}$ vs. T [55Cro]. $\kappa_{\perp c}$: dielectric constant for electric field perpendicular to c.

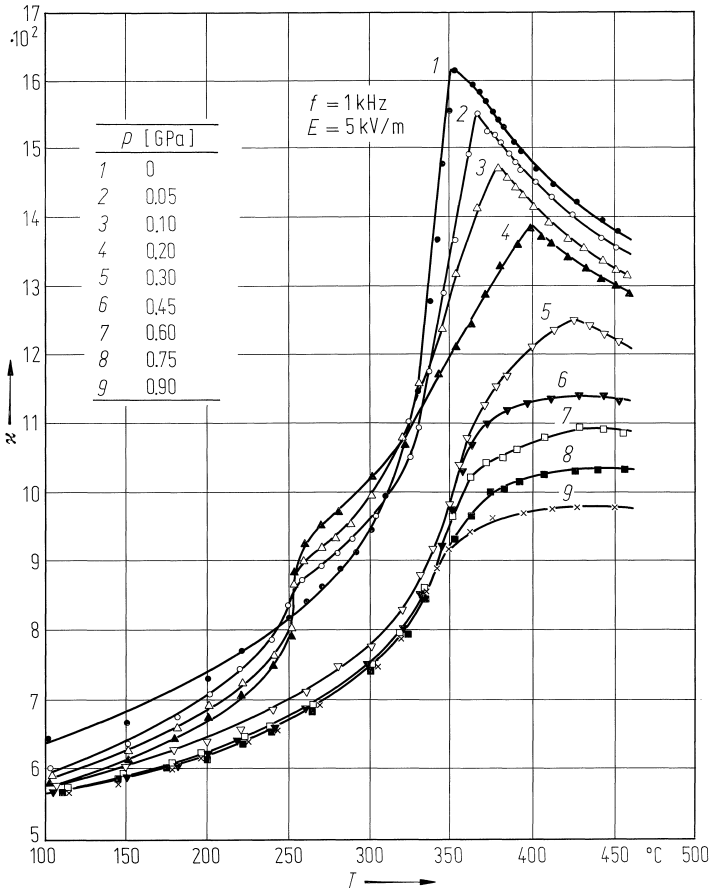

Fig. 1A-1-005. $NaNbO_3$. κ vs. T [80Pis1]. Parameter: p.

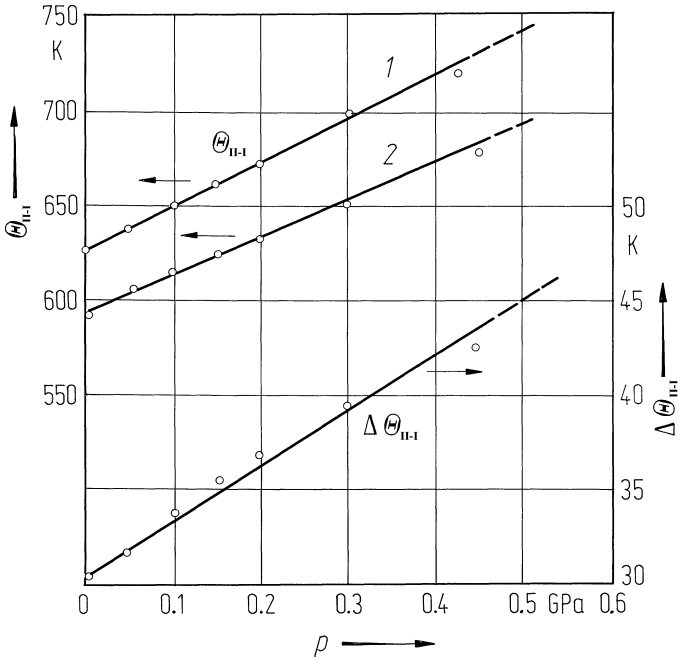

Fig. 1A-1-006. $NaNbO_3$. Θ_{II-I}, $\Delta\Theta_{II-I}$ vs. p [80Pis1]. Curve *1*: Θ_{II-I} on heating, curve *2*: Θ_{II-I} on cooling. $\Delta\Theta_{II-I}$: thermal hysteresis of Θ_{II-I} during heating and cooling processes.

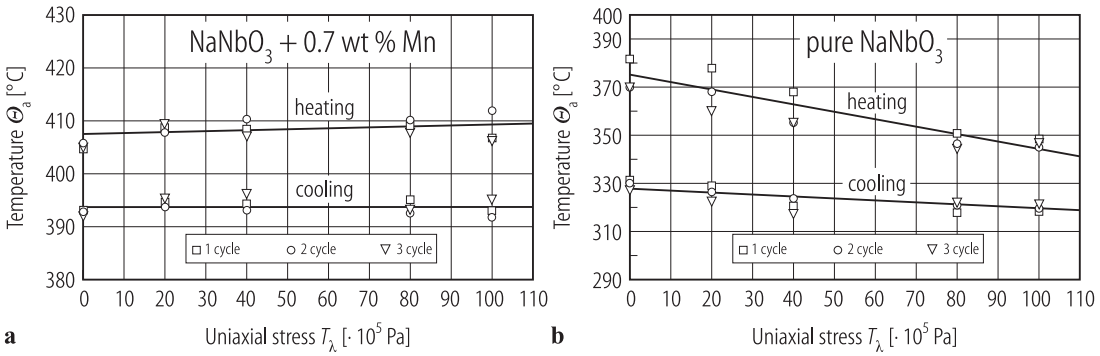

Fig. 1A-1-007. $NaNbO_3$, $NaNbO_3$ with 0.7 wt % Mn additives (ceramics). Θ_a vs. T_λ [94Mol]. T_λ: uniaxial stress. Heating and cooling cycles were repeated three times under constant stress.

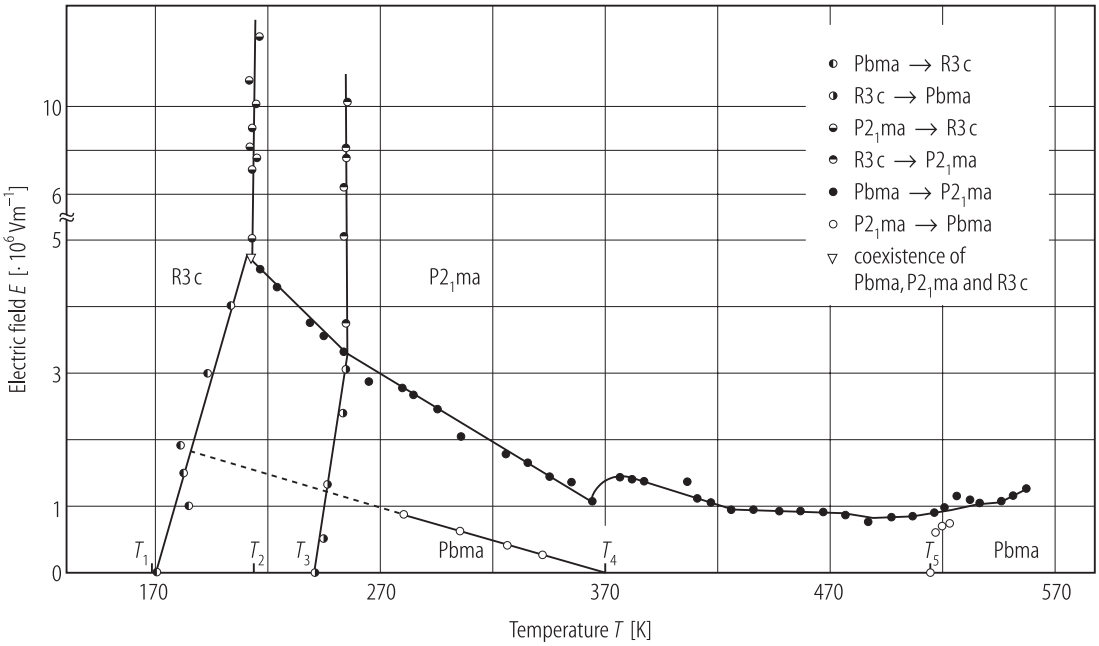

Fig. 1A-1-008. $NaNbO_3$. E–T phase diagram [87Zhe]. E: electric field normal to orthorhombic c-axis of phase IV (Pbma).

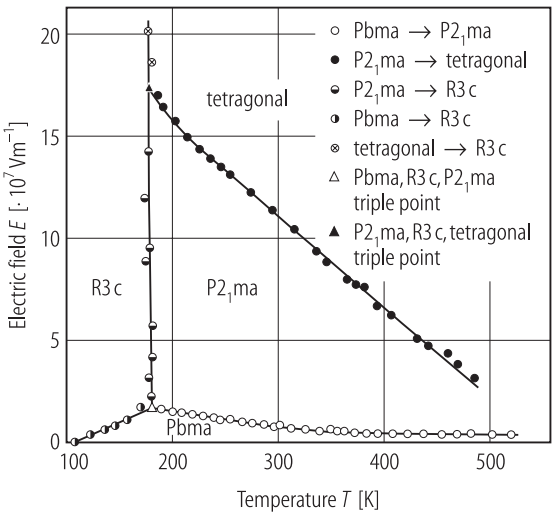

Fig. 1A-1-009. $NaNbO_3$. *E*–*T* phase diagram [90Uli]. *E*: electric field normal to orthorhombic *c*-axis of phase IV (Pbma).

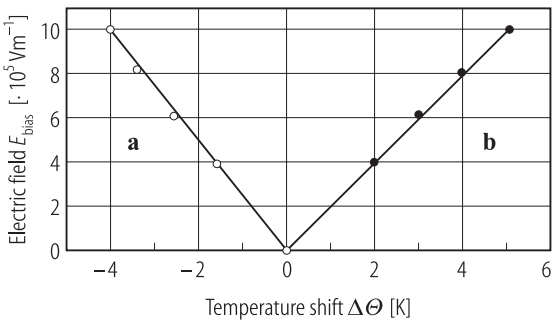

Fig. 1A-1-010. $NaNbO_3$ (**a**), $(Na_{0.98}Li_{0.02})NbO_3$ (**b**) (ceramics). $\Delta\Theta$ vs. E_{bias} [86Ism]. $\Delta\Theta$: shift of Θ_{II-I}.

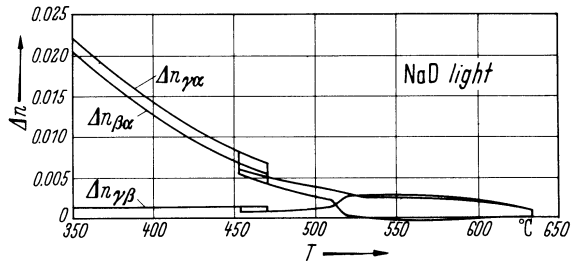

Fig. 1A-1-011. $NaNbO_3$. Δn vs. T [55Cro]. $\Delta n_{\gamma\alpha} = n_\gamma - n_\alpha$, $\Delta n_{\beta\alpha} = n_\beta - n_\alpha$, $\Delta n_{\gamma\beta} = n_\gamma - n_\beta$. See also [55Jon].

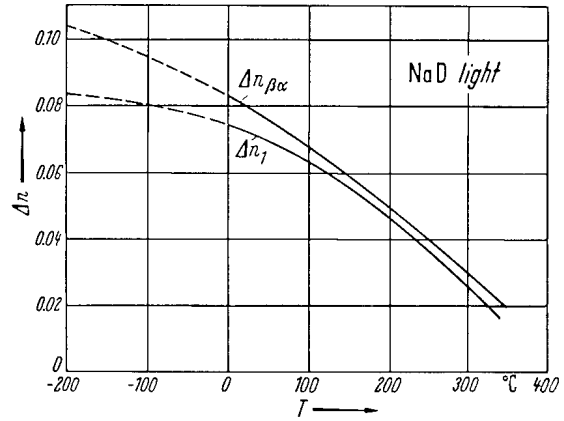

Fig. 1A-1-012. $NaNbO_3$. Δn vs. T [55Cro]. $\Delta n_{\beta\alpha} = n_\beta - n_\alpha$, $\Delta n_1 = n_\gamma - n_{(\alpha+\beta)/2}$. $n_{(\alpha+\beta)/2}$: refractive index along 45^o bisector of the ellipse in $\alpha\beta$ section of indicatrix.

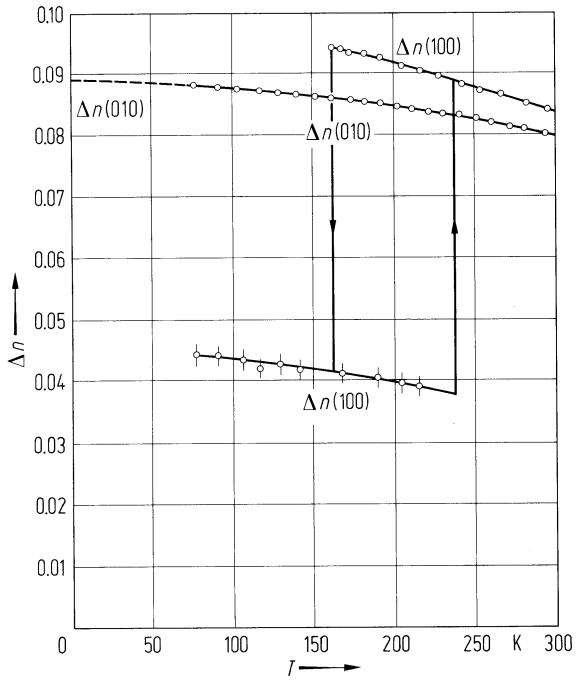

Fig. 1A-1-013. $NaNbO_3$. Δn vs. T [78Sei]. Measurements were made on planes correlated to the pseudocubic axes. λ = 589 nm.

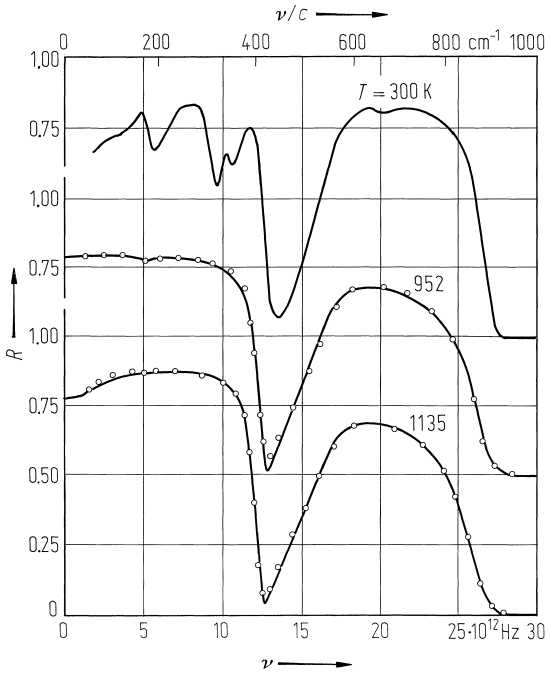

Fig. 1A-1-014. $NaNbO_3$. R vs. ν [82Ger]. Parameter: T. R: infrared reflectivity. Curves show the fits of data by a dielectric function of the following form: $\kappa(\omega) = \kappa_\infty \Pi_j [(\Omega_{jLO}^2 - \omega^2 + i\,\omega\,\gamma_{jLO}) / (\Omega_{jTO}^2 - \omega^2 + i\,\omega\,\gamma_{jTO})]$.

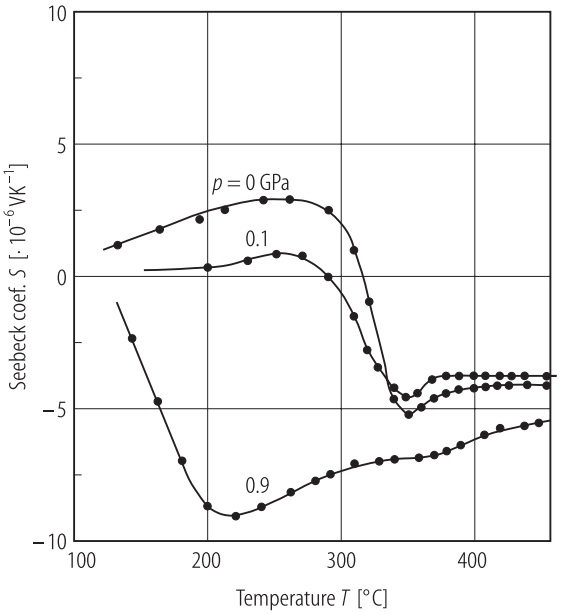

Fig. 1A-1-015. $NaNbO_3$. S vs. T [80Pis2]. Parameter: p.
S: Seebeck coefficient.

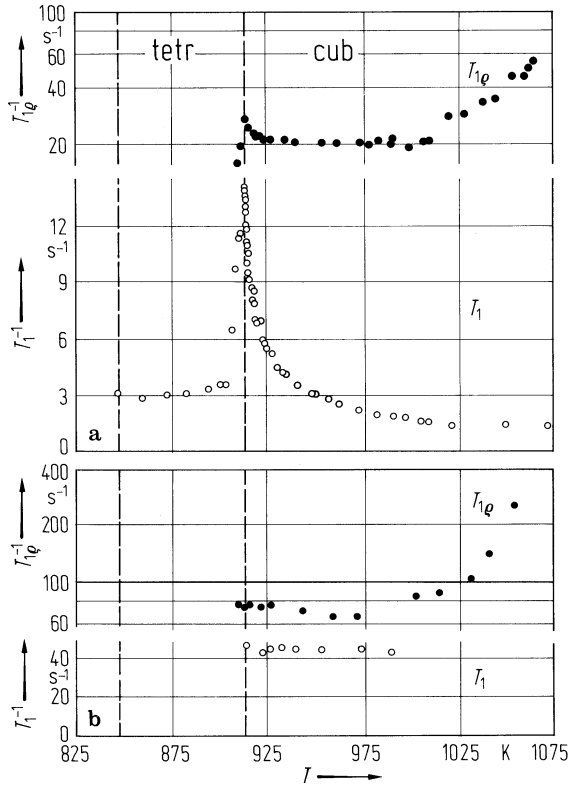

Fig. 1A-1-016. $NaNbO_3$. T_1^{-1}, $T_{1\rho}^{-1}$ vs. T [75Avo]. T_1: quadrupole spin-lattice relaxation time in laboratory frame, $T_{1\rho}$: that in rotating frame. **(a)**: ^{23}Na, **(b)**: ^{93}Nb. See also [74Avo].

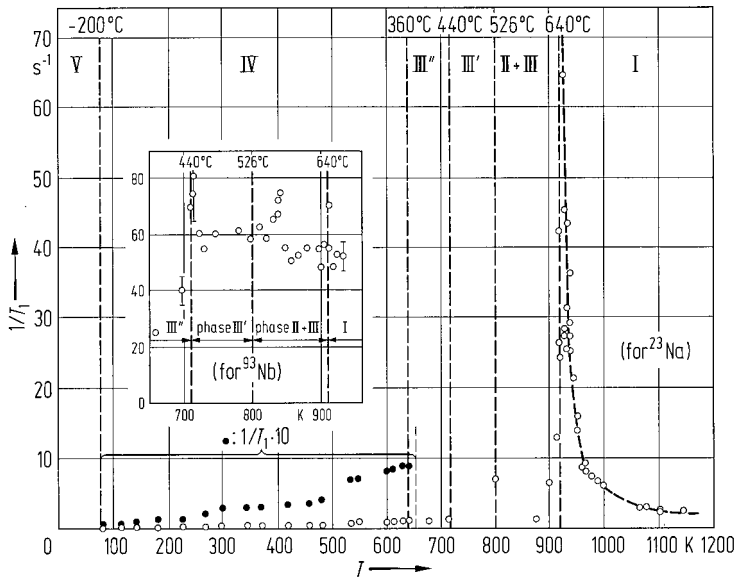

Fig. 1A-1-017. $NaNbO_3$. $1/T_1$ vs. T [72Bon]. T_1: ^{23}Na spin-lattice relaxation time. ν = 22 MHz. Insert: indicative data of $1/T_1$ for ^{93}Nb.

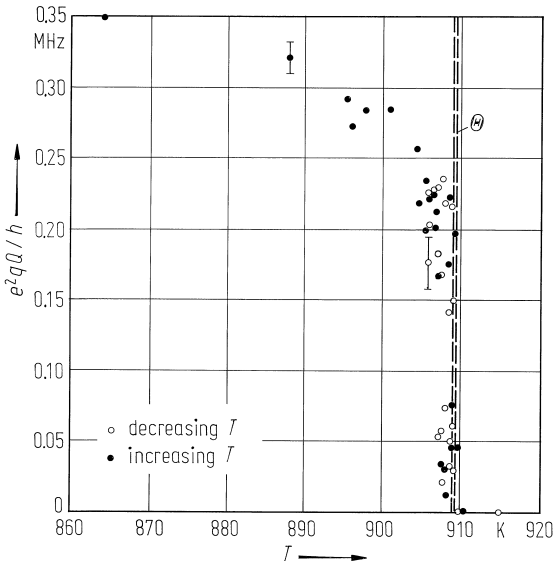

Fig. 1A-1-018. $NaNbO_3$. e^2qQ/h vs. T [82DAr]. e^2qQ/h: ^{23}Na quadrupole coupling constant. Vertical lines indicate transition temperatures.

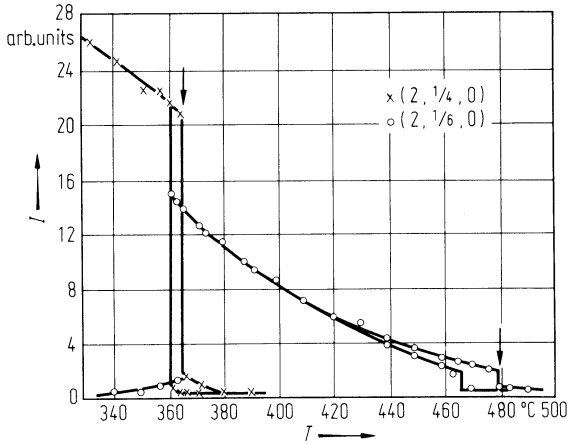

Fig. 1A-1-019. $NaNbO_3$. *I* vs. *T* [73Ish]. *I*: X-ray reflection intensity. Bragg reflections are indexed on the basis of cubic cell of phase I.

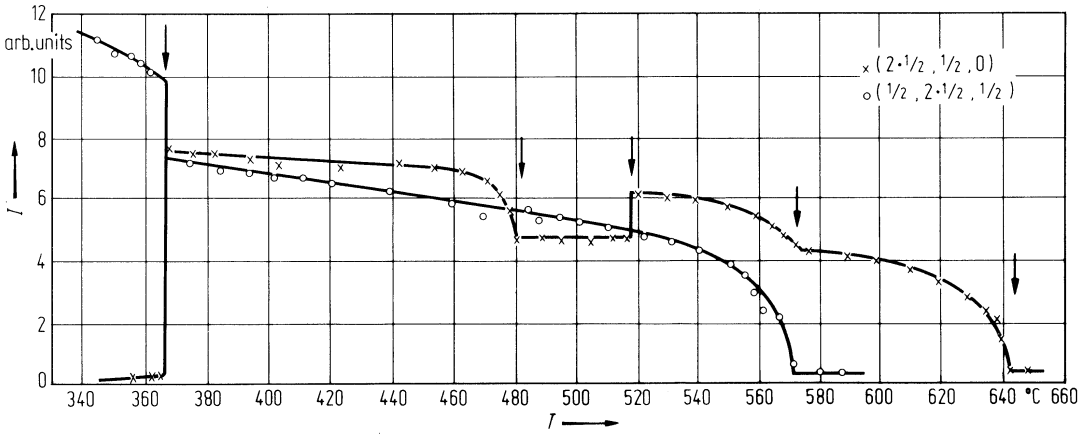

Fig. 1A-1-020. $NaNbO_3$. *I* vs. *T* [73Ish]. *I*: X-ray reflection intensity. Bragg reflections are indexed on the basis of cubic cell of phase I. Arrows indicate phase transition temperatures.

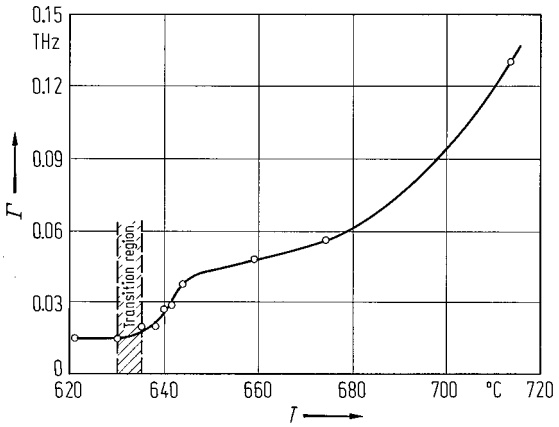

Fig. 1A-1-021. $NaNbO_3$. Γ vs. T [76Den]. Inelastic neutron scattering. Γ: full width at half maximum of quasielastic peak at M-point.

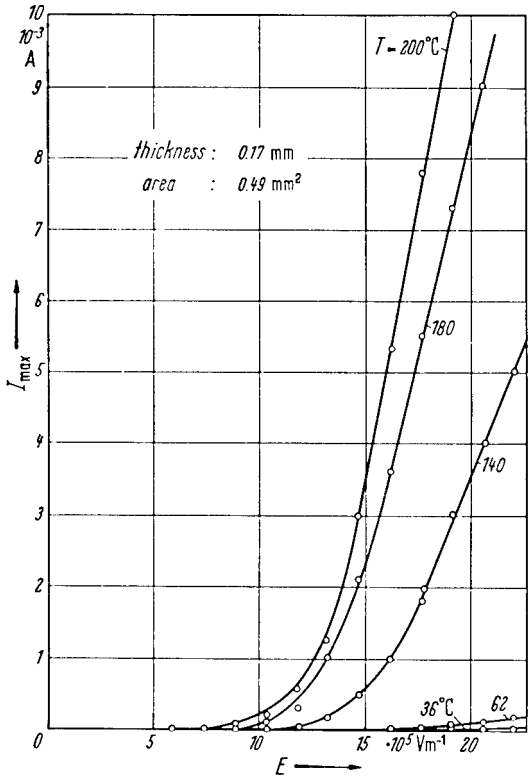

Fig. 1A-1-022. $Na(Nb_{0.8}V_{0.2})O_3$. I_{max} vs. E [60Pul]. Parameter: T. I_{max}: maximum switching current. Thickness: 0.17 mm, area: 0.49 mm².

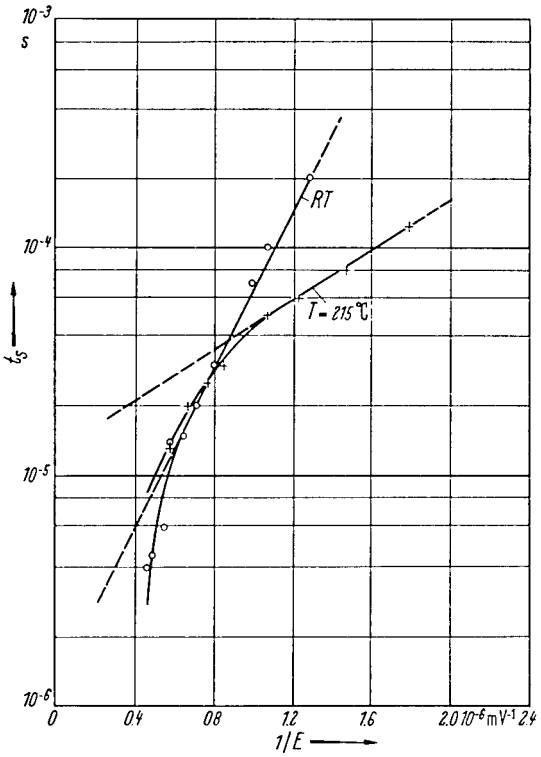

Fig. 1A-1-023. $(Na_{0.9}Ag_{0.1})NbO_3$. t_s vs. $1/E$ [60Pul].
t_s: switching time.

References

51Mat Matthias, B.T., Remeika, J.P.: Phys. Rev. **82** (1951) 727.
51Vou Vousden, P.: Acta Crystallogr. **4** (1951) 545.
51Woo Wood, E.A.: Acta Crystallogr. **4** (1951) 353.
54Shi Shirane, G., Newnham, R.E., Pepinsky, R.: Phys. Rev. **96** (1954) 581.
55Cro Cross, L.E., Nicholson, B.J.: Philos. Mag. [7] **46** (1955) 453.
55Jon Jona, F., Shirane, G., Pepinsky, R.: Phys. Rev. **97** (1955) 1584.
60Pul Pulvari, C.F.: Phys. Rev. **120** (1960) 1670.
61Wel Wells, M., Megaw, H.D.: Proc. Phys. Soc. (London) **78** (1961) 1258.
62Mil Miller, R.C., Wood, E.A., Remeika, J.P., Savge, A.: J. Appl. Phys. **33** (1962) 1623.
62Woo Wood, E.A., Miller, R.C., Remeika, J.P.: Acta Crystallogr. **15** (1962) 1273.
64Per Perry, C.H., Khanna, B.N., Rupprecht, G.: Phys. Rev. **135** (1964) A408.
66Abr Abrahams, S.C., Reddy, J.M., Bernstein, J.L.: J. Phys. Chem. Solids **27** (1966) 997.
67Kat Katz, L., Megaw, H.D.: Acta Crystallogr. **22** (1967) 639.
69Sak Sakowski-Cowley, A.C., Lukaszewicz, K., Megaw, H.D.: Acta Crystallogr., Sect. B **25** (1969) 851.
71Com Comes, R., Denoyer, F., Lambert, M.: J. Phys. (Paris) **32**, Suppl. C-5a (1971) 195.
71Dar Darlington, C.N.W.: Thesis, University of Cambridge, 1971.
71Sak Sakowski-Cowely, A.C.: Thesis, University of Cambridge, 1971.
72Aht Ahtee, M., Glazer, A.M., Megaw, H.D.: Philos. Mag. [8] **26** (1972) 995.
72Bon Bonera, G., Borsa, F., Rigamonti, A.: J. Phys. (Paris) Colloque **33**, Suppl. C-2 (1972) 195.
72Gla Glazer, A.M., Megaw, H.D.: Philos. Mag. [8] **25** (1972) 1119.
73Dar Darlington, C.N.W., Megaw, H.D.: Acta Crystallogr., Sect. B **29** (1973) 2171.
73Ish Ishida, K., Honjo, G.: J. Phys. Soc. Jpn. **34** (1973) 1279.
74Avo Avogadro, A., Bonera, G., Borsa, F., Rigamonti, A.: Phys. Rev. B **9** (1974) 3905.
74Daw Dawson, R.D., Elwell, D., Brice, J.C.: J. Cryst. Growth **23** (1974) 65.
74Hew Hewat, A.: Ferroelectrics **7** (1974) 83.
75Avo Avogadro, A., Bonera, G., Rigamonti, A.: J. Magn. Reson. **20** (1975) 399.
75Gei Geifman, I.N., Grachev, V.G., Krulikovskii, B.K.: Fiz. Tverd. Tela **17** (1975) 1862; Sov. Phys. Solid State (English Transl.) **17** (1975) 1225.
76Den Denoyer, F., Lambert, M., Comes, R., Currat, R.: Solid State Commun. **18** (1976) 441.
76Gei Geifman, I.N., Glinchuk, M.D., Bykov, I.P., Rozhko, V.S., Krulikovskii, B.K.: Fiz. Tverd. Tela **18** (1976) 2642; Sov. Phys. Solid State (English Transl.) **18** (1976) 1541.
77Rae1 Raevskii, I.P., Malitskaya, M.A., Prokopalo, O.I., Smotrakov, V.G., Fesenko, E.G.: Fiz. Tverd. Tela **19** (1977) 492; Sov. Phys. Solid State (English Transl.) **19** (1977) 283.
77Rae2 Raevskii, I.P., Malitskaya, M.A., Prokopalo, O.I., Smotrakov, V.G., Fesenko, E.G., Tsikhotskii, E.S.: Fiz. Tverd. Tela **19** (1977) 2033; Sov. Phys. Solid State (English Transl.) **19** (1977) 1189.
78Han Handerek, J., Wrobel, Z., Wojcik, K., Ujma, Z.: Ferroelectrics **18** (1978) 127.
78Sei Seidel, P., Bomas, H., Hoffmann, W.: Ferroelectrics **18** (1978) 243.
79Rae Raevskii, I.P., Malitskaya, M.A., Prokopalo, O.I., Smotrakov, V.G., Fesenko, E.G.: Fiz. Tverd. Tela **21** (1979) 1232; Sov. Phys. Solid State (English Transl.) **21** (1979) 715.
79Tur Turik, A.V., Shevchenko, N.B., Zhestkov, V.F., Smotrakov, V.G., Fesenko, E.G.: Fiz. Tverd. Tela **21** (1979) 1224; Sov. Phys. Solid State (English Transl.) **21** (1979) 710.
80Pis1 Pisarski, M.: Acta Phys. Polon. A **57** (1980) 693.
80Pis2 Pisarski, M.: Phys. Status Solidi (b) **101** (1980) 635.
80Smo Smotrakov, V.G., Raevskii, I.P., Malitskaya, M.A., Zhelnova, O.A., Leont'ev, N.G., Prokopalo, O.I., Fesenko, E.G.: Izv. Akad. Nauk SSSR, Neorg. Mater. **16** (1980) 1065; Inorg. Mater. (English Transl.) **16** (1980) 740.

80Tan Tanaka, J., Tsukioka, M., Miyazawa, Y., Mori, Y., Shimizu, S.: Solid State Commun. **34** (1980) 221.
81Pro Prokopalo, O.I., Raevskii, I.P., Malitskaya, M.A., Popov, Yu.M., Smotrakov, V.G., Fesenko, E.G.: Ferroelectrics **34** (1981) 57.
82DAr D'Ariano, G., Aldrovandi, S., Rigamonti, A.: Phys. Rev. B **25** (1982) 7044.
82Gei Geifman, I.N., Bykov, I.P., Krulikovskii, B.K.: Fiz. Tverd. Tela **24** (1982) 3161; Sov. Phys. Solid State (English Transl.) **24** (1982) 1793.
82Ger Gervais, F., Servoin, J.L., Baumard, J.F., Denoyer, F.: Solid State Commun. **41** (1982) 345.
83Zhe Zhelnova, O.A., Fesenko, O.E., Smotrakov, V.G., Zaitsev, S.M.: Kristallografiya **28** (1983) 932; Sov. Phys. Crystallogr. (English Transl.) **28** (1983) 552.
84Mol Molak, A., Pichet, J.: Acta Phys. Polon. A **66** (1984) 251.
85Mol Molak, A., Jelonex, M.: J. Phys. Chem. Solids **46** (1985) 21.
86Ism Ismailzade, I.G., Hagenmuller, P., Samedov, O.A., Ravez, J., Ismailov, R.M.: Izv. Akad. Nauk SSSR, Neorg. Mater. **22** (1986) 846; Inorg. Mater. (English Transl.) **22** (1986) 745.
87Zhe Zhelnova, O.A., Fesenko, O.E.: Ferroelectrics **75** (1987) 469.
88Che Chen, J., Feng, D.: Phys. Status Solidi (a) **109** (1988) 171.
88Dec Dec, J.: Ferroelectrics **81** (1988) 123.
88Mol Molak, A.: Ferroelectrics **80** (1988) 27.
90Uli Ulinzheyev, A.V., Fesenko, E.G., Smotrakov, V.G.: Ferroelectrics Lett. **12** (1990) 17.
91Bak Bak, W., Kus, C., Ptak, W.S.: Ferroelectrics **115** (1991) 105.
94Kin King-Smith, R.D., Vanderbit, D.: Phys. Rev. B **49** (1994) 5828.
94Mol Molak, A., Pawelczyk, M., Kwapuli'nski, J.: J. Phys. Condens. Matter **6** (1994) 6833.